Progress In Electromagnetics Research Letters, Vol. 56, 1–7, 2015

Bandpass Filters with Improved Selectivity Based on Dual-Mode Ring Resonators

Wenjie Feng*, Xin Gao, and Wenquan Che

Abstract—Two novel microstrip bandpass filters with improved selectivity based on dual-mode ring resonators are proposed. Tow and four transmission zeros close to the passband are realized to improve the selectivity for the passband. Sixth-order passband is realized with two open/shorted stubs and a dual-mode ring resonator. The transmission zeros near the passband can be adjusted conveniently by changing the characteristic impedances of the coupled lines. For demonstration, two planar bandpass filters (3-dB bandwidths 20.9%, 20.2%) are designed and fabricated.

1. INTRODUCTION

As one of the typical microwave filters, dual-mode bandpass filter has many attractive advantages such as low radiation loss, high Q factor, two inherent transmission zeros close to the passband, compact size and sharp rejection shirts [1, 2]. Using different perturbations, ring resonators with open stubs and notches were used to design different bandpass filters, diplexer and power dividers with high selectivity and high isolation [3–14]. In [15, 16], dual-mode bandpass filters without any perturbations using sided-coupled lines were proposed, the bandwidth, transmission zeros frequencies of the dual-mode resonator can be simply controlled by changing the characteristic impedance of the couple lines, however, numbers of ring resonators should be used to increase the passband-order, and the transmission zeros out-of-stopband don't increase.

In this paper, two novel bandpass filters with improved selectivity based on dual-mode ring resonators are proposed. Six-order passband can be realized by only a ring resonator, and two/four transmission zeros close to the passband can be used to improve the passband selectivity. The out-of-band transmission zeros can be adjusted conveniently by changing the even/odd-mode coupled line impedances. Two prototypes of the bandpass filters operating at 3.1 GHz are constructed on the dielectric substrate with $\varepsilon_r = 2.65$, $h = 1.0\,\text{mm}$, and $\tan\delta = 0.003$. All the structures are simulated with simulated with ANSYS Designer v3.0 and ANSYS HFSS v.11.0.

2. ANALYSIS AND DESIGN OF PROPOSED BANDPASS FILTERS

2.1. Bandpass Filter with Two Transmission Zeros

Figures 1(a)–(b) show the dual-mode filter in [15], and the proposed dual-mode bandpass filter with two transmission zeros, a dual-mode ring resonator is attached to two quarter-wavelength side-coupled lines (electrical length θ, even/odd-mode characteristic impedance Z_{e1}, Z_{o1}). Two open coupled lines (Z_{e1}, Z_{o1}, θ) with shorted loaded stubs (Z_1, θ) are located in the middle of the bandpass filter. Two microstrip lines with characteristic impedance $Z_0 = 50\,\Omega$ are connected to Ports 1, 2.

Received 26 July 2015, Accepted 17 August 2015, Scheduled 30 August 2015
* Corresponding author: Wenjie Feng (fengwenjie1985@163.com).
The authors are with the Department of Communication Engineering, Nanjing University of Science & Technology, Nanjing, China.

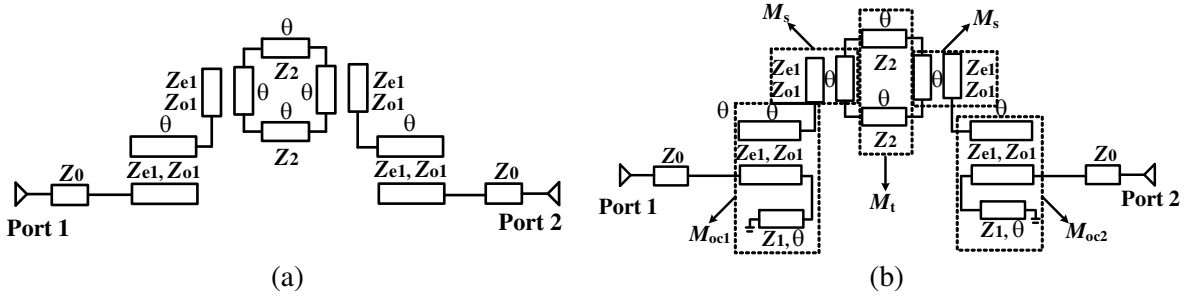

Figure 1. (a) Bandpass filter in Ref. [10], (b) proposed bandpass filter with two transmission zeros.

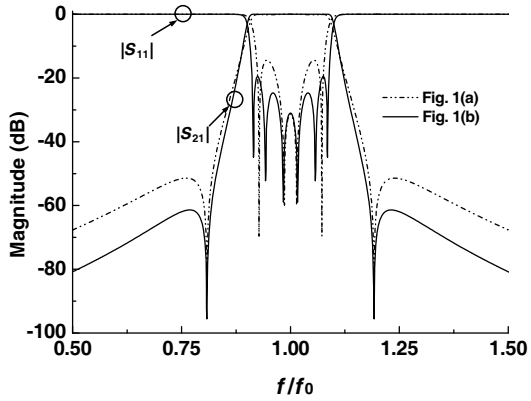

Figure 2. Simulated frequency responses of Figs. 1(a)–(b). ($Z_0 = 50\,\Omega$, $Z_1 = 118\,\Omega$, $Z_2 = 120\,\Omega$, $Z_{e1} = 180\,\Omega$, $Z_{o1} = 110\,\Omega$).

The simulated results of Figs. 1(a)–(b) are shown in Fig. 2. Due to the two shorted loaded stubs (Z_1), the passband-order can be increased from fourth to sixth, and the locations of two transmission zeros realized by the dual-mode resonator do not change. The $ABCD$ matrix of the bandpass filter circuit for Fig. 1(b) can be defined as $M_{oc1} \times M_s \times M_t \times M_s \times M_{oc2}$ ($M_{co1/2}$-coupled lines with shorted stubs, M_s-side-coupled lines, M_t-center two transmission lines), and the matrices of the coupled lines and stubs can be obtained from [17]. After $ABCD$-, Y- and S-parameter conversions, when $S_{21} = 0$, two transmission zeros can be obtained:

$$\theta_{tz1} = \arccos\sqrt{\frac{Z_{e1} + Z_{o1} - 2Z_2}{Z_{e1} + Z_{o1} + 2Z_2}}, \quad \theta_{tz2} = \pi - \theta_{tz1} \tag{1}$$

In addition, the transmission poles in the passband can be calculated when $S_{11} = 0$. When Z_0 is fixed, six roots for $S_{11} = 0$ can be found by properly choosing the relationships of Z_1, Z_2, Z_{e1}, Z_{o1}, and then six transmission poles in the passband can be achieved. The two transmission poles near the passband edge are realized by the dual-mode ring resonator, and the two poles near the center frequency (f_0) are produced by the open coupled lines [15].

The simulated frequency responses of Fig. 1(b) are shown in Fig. 3(a). Two transmission zeros (f_{tz1}, f_{tz2}) close to the passband can be produced by the dual-mode ring resonator [10]. In addition, for a high selectivity bandpass filter, the 3-dB bandwidth (Δf, %), maximal $|S_{21}|$ (T_{stop}, dB) in the stopband and the maximal in-band $|S_{11}|$ (T_{pass}, dB) referring to the responses in Fig. 3(a) are the mainly concerned filter characteristics, the corresponding levels of Δf, T_{stop} and T_{pass} versus Z_1, Z_2, Z_{e1} and Z_{o1} are shown and listed in Fig. 3(b) and Table 1, and the 3-dB bandwidth of Δf and T_{pass} decreases as Z_1, Z_2 increases, the T_{stop} increases as Z_1, Z_2 increases. The two transmission zeros (f_{tz1}, f_{tz2}) move towards f_0 with the increase of the sum for Z_{e1}, Z_{o1}. In this way, a sixth-order passband with two transmission zeros for the bandpass filter can be easily realized.

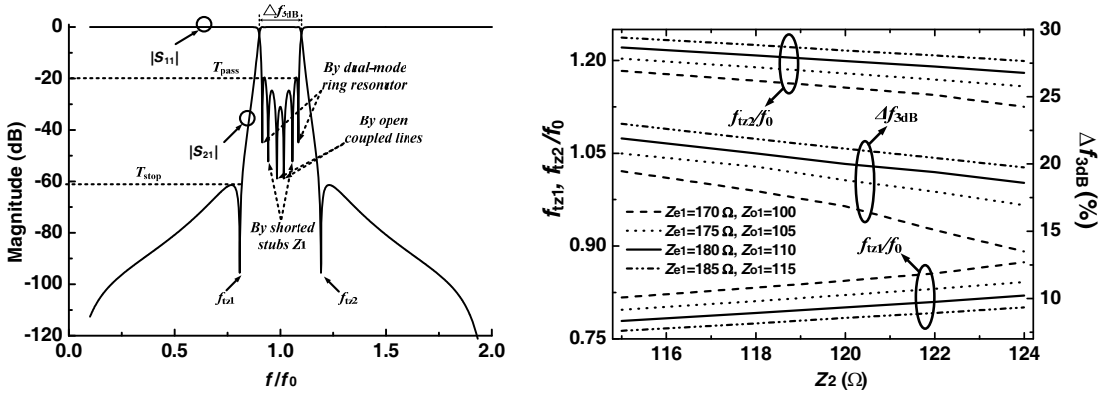

(a) (b)

Figure 3. Simulated frequency responses of Fig. 1(b). (a) $|S_{21}|\&|S_{11}|$, $Z_0 = 50\,\Omega$, $Z_1 = 118\,\Omega$, $Z_2 = 120\,\Omega$, $Z_{e1} = 180\,\Omega$, $Z_{o1} = 110\,\Omega$, (b) f_{tz1}, f_{tz2}/f_o, Δf versus Z_{e1}, Z_{o1}, Z_2, $Z_0 = 50\,\Omega$, $Z_1 = 118\,\Omega$.

Table 1. Δf, T_{pass} and T_{stop} of Fig. 3(a) versus Z_1, Z_2.

$Z_{e1} = 180\,\Omega$ $Z_{o1} = 110\,\Omega$		Z_1								
		$110\,\Omega$			$115\,\Omega$			$120\,\Omega$		
		Δf	T_{pass}	T_{stop}	Δf	T_{pass}	T_{stop}	Δf	T_{pass}	T_{stop}
Z_2	$115\,\Omega$	22%	−9.5	−68.5	21.2%	−10.3	−66.5	20.4%	−11.6	−63.2
	$120\,\Omega$	21%	−17.4	−64.2	20.5%	−19.6	−62.3	19.2%	−20.4	−60.6
	$125\,\Omega$	18%	−11.2	−60.1	17.2%	−12.7	−58.5	16.4%	−13.9	−57.7

2.2. Bandpass Filter with Four Transmission Zeros

Figure 4(a) shows ideal transmission circuit of the bandpass filter with four transmission zeros, and two half-wavelength open stubs (Z_1, 2θ) are shunted connected to the open coupled lines (Z_{e1}, Z_{o1}, θ). The $ABCD$ matrix of the bandpass filter for Fig. 4(a) can be also defined as $M_{oc1} \times M_s \times M_t \times M_s \times M_{oc2}$, and after $ABCD$-, Y- and S-parameter conversions, when $S_{21} = 0$, besides the two transmission zeros (f_{tz1}, f_{tz2}) produced by the dual-mode ring resonator, another two transmission zeros created by the two half-wavelength open stubs can be achieved as:

$$\theta_{tz3} = 0.5\pi, \quad \theta_{tz4} = 1.5\pi \tag{2}$$

The simulated frequency responses of Fig. 4(a) are shown in Fig. 4(b). Compared with the bandpass filter of Fig. 3(a), the two transmission zeros f_{tz3}, f_{tz4} can be used to further improve the passband selectivity. In addition, the locations of two transmission zeros f_{tz1}, f_{tz2} do not change with Z_1, and the locations of two transmission zeros f_{tz3}, f_{tz4} do not change with Z_{e1} andZ_{o1}. So besides the advantage for bandpass filter with two transmission zeros, the two transmission zeros (f_{tz3}, f_{tz4}) can be seen as another independently adjustable parameters to improve the transmission characteristic for the bandpass filter with four transmission zeros.

2.3. Proposed Two Bandpass Filters

To clarify the proposed filters design, the design procedures of the two bandpass filters can be summarized as:

(1) Based on Equations (1)–(2), choose the desired center frequency f_0 of the bandpass filters, determine the two/four transmission zeros locations close to the passband;

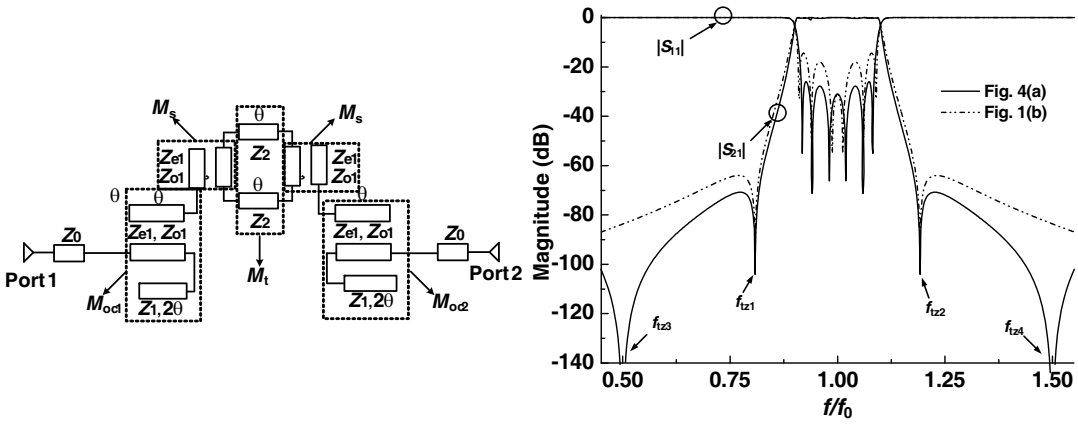

Figure 4. (a) Proposed bandpass filter with four transmission zeros, (b) simulated frequency responses of Figs. 1(a) and 4(a). (Z_0= 50 Ω, $Z_1 = 118/130\,\Omega$, $Z_2 = 125\,\Omega$, $Z_{e1} = 180\,\Omega$, $Z_{o1} = 110\,\Omega$).

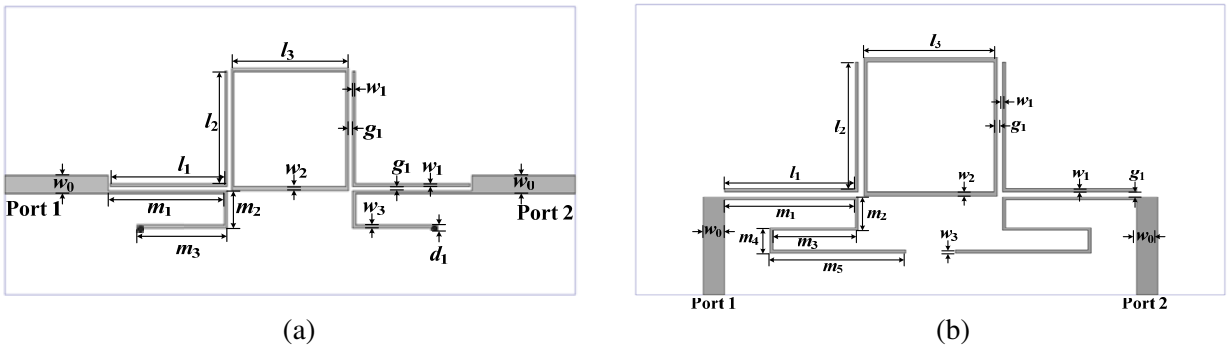

Figure 5. Geometries of the proposed bandpass filters. (a) Two transmission zeros, (b) four transmission zeros.

(2) Adjust the shorted/open loaded stubs (Z_1) and transmission lines (Z_2) to realize a sixth-order passband for the two bandpass filters, choose the desired bandwidth for the filter (3-dB bandwidth greater than 20%, ($|S_{11}| < -15\,\text{dB}$), out-of-band harmonic suppression ($|S_{21}| < -20\,\text{dB}$);

(3) Further optimize the values of Z_{e1}, Z_{e1} to realize better in-band and out-of-band transmission characteristics of the two bandpass filters, carry out full-wave electromagnetic simulation and dimension optimization in the commercial software of HFSS.

Referring to the above discussions and simulated results, the 3-dB bandwidths of the two bandpass filters are chosen as 21.5% and 21%, and the final parameters for the filters of Fig. 1(b), 4(a) are listed as below: $Z_0 = 50\,\Omega$, $Z_1 = 118\,\Omega$, $Z_2 = 121\,\Omega$, $Z_{e1} = 181\,\Omega$, $Z_{o1} = 109\,\Omega$; $Z_0 = 50\,\Omega$, $Z_1 = 130\,\Omega$, $Z_2 = 125\,\Omega$, $Z_{e1} = 182\,\Omega$, $Z_{o1} = 112\,\Omega$. The structure parameters for two bandpass filters shown in Fig. 5 are: $l_1 = 17.2\,\text{mm}$, $l_2 = 17.0\,\text{mm}$, $l_3 = 17.1\,\text{mm}$, $m_1 = 17.2\,\text{mm}$, $m_2 = 5.5\,\text{mm}$, $m_3 = 12.4\,\text{mm}$, $w_0 = 2.7\,\text{mm}$, $w_1 = 0.2\,\text{mm}$, $w_2 = 0.42\,\text{mm}$, $w_3 = 0.47\,\text{mm}$, $g_1 = 0.55\,\text{mm}$, $d_1 = 0.7\,\text{mm}$; $l_1 = 17.1\,\text{mm}$, $l_2 = 17.0\,\text{mm}$, $l_3 = 17.1\,\text{mm}$, $m_1 = 17.26\,\text{mm}$, $m_2 = 4.2\,\text{mm}$, $m_3 = 11.0\,\text{mm}$, $m_4 = 3.2\,\text{mm}$, $m_5 = 17.5\,\text{mm}$, $w_0 = 1.37\,\text{mm}$, $w_1 = 0.2\,\text{mm}$, $w_2 = 0.42\,\text{mm}$, $w_3 = 0.2\,\text{mm}$, $g_1 = 0.59\,\text{mm}$.

Figures 6–7 illustrate the photographs, simulated and measured results of the two bandpass filters with two/four transmission zeros. For the bandpass filter with two transmission zeros, two simulated transmission zeros are located at 2.45, 3.6 GHz, the in-band insertion loss is less than 1.65 dB with 3-dB bandwidth approximately 21.9% (2.75–3.43 GHz); for the bandpass filters with four transmission zeros, four simulated transmission zeros are located at 1.65, 2.55, 3.58, and 4.14 GHz, the in-band return loss is greater than 13 dB from 2.76 to 3.44 GHz with 3-dB bandwidth approximately 20.9% (2.77–3.42 GHz).

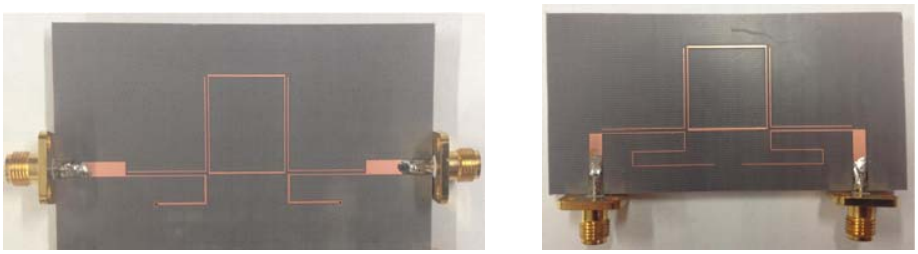

(a) (b)

Figure 6. Photographs of the proposed bandpass filters. (a) Two transmission zeros, (b) four transmission zeros.

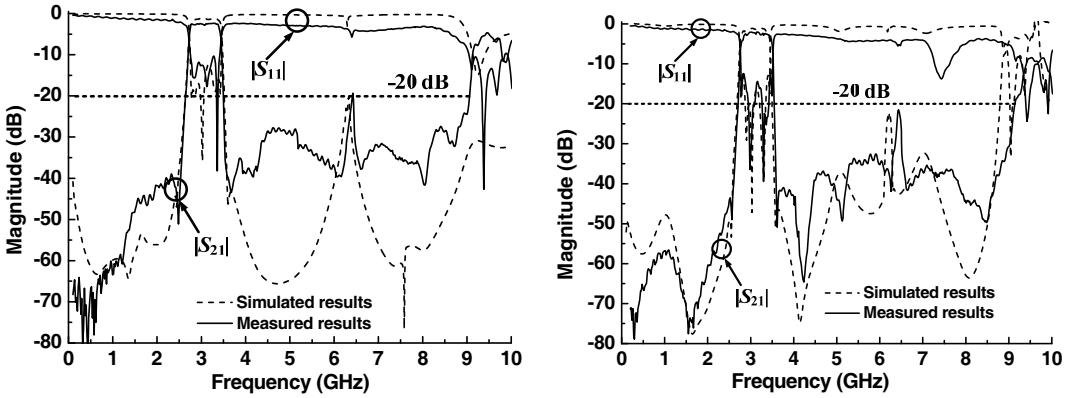

Figure 7. Measured and simulated results of the proposed bandpass filters. (a) Two transmission zeros, (b) four transmission zeros.

3. MEASURED RESULTS AND DISCUSSIONS

The measured results of the two bandpass filters are also illustrated in Figs. 7(a)–(b). Good agreements can be observed between the simulation and experiments. For the bandpass filter of Fig. 6(a), the 3-dB bandwidth is 20.9% (2.74–3.39 GHz) with return loss greater than 10.5 dB (2.78–3.37 GHz), three measured transmission zeros are located at 2.48, 3.68 and 4.3 GHz, over 20-dB upper stopband is realized from 3.56 to 9.06 GHz ($2.92f_0$). For the bandpass filter of Fig. 6(b), five measured transmission zeros are located at 1.62, 2.56, 3.61, 4.23 and 5.13 GHz, the 3-dB bandwidth is 20.2% (2.8–3.42 GHz) with insertion loss less than 2.55 dB (2.88–3.39 GHz), over 20-dB upper stopband is realized from 3.54 to 9.14 GHz ($2.95f_0$). The second harmonic around 6.35 GHz is mainly due to the desynchronization between the quarter-wavelength lines in the resonator [15]. In addition, the slight frequency discrepancies of the transmission zeros in the upper stopband, and larger insertion loss for the passband between the measured and simulated results are mainly caused by the imperfect soldering skill of the shorted stubs and folded transmission lines of the bandpass filters.

For comparisons, Table 2 illustrates the measured results for some bandpass filter structures. Obviously, compared with the other filters [3–15], three and five transmission zeros close to the passband are realized with only a ring resonator, and the upper stopband for the filter stretches up to $2.92f_0/2.95f_0$ ($|S_{21}| < -20$ dB). Moreover, the bandwidth of the proposed filters can be further extended by using interdigital coupled lines as [5].

Table 2. Comparison of for several bandpass filter structures.

Filter Structures	Transmission zeros, $\|S_{21}\|$ 0-2f_0, (f_0)	3-dB bandwidth	Numbers of ring resonator	Effective circuit size ($\lambda_0 \times \lambda_0$)	Upper Stopband, $\|S_{21}\|$, dB
Ref. [3]	4 (4.0 GHz)	11.2%	2	0.35×0.35	< -20, $(1.60f_0)$
Ref. [5]	3 (4.0 GHz)	64.0%	1	0.65×0.25	< -25, $(2.00f_0)$
Ref. [6]	5 (3.0 GHz)	79.0%	1	0.50×0.25	< -25, $(2.60f_0)$
Ref. [7]	6 (5.0 GHz)	10.7%	2	0.50×0.30	< -20, $(1.40f_0)$
Ref. [8]	3 (6.8 GHz)	103%	1	0.75×0.25	< -20, $(2.40f_0)$
Ref. [9]	4 (7.7 GHz)	123%	1	0.25×0.25	< -15, $(2.40f_0)$
Ref. [15]	3 (2.0 GHz)	10.0%	1	0.75×0.30	< -20, $(2.80f_0)$
These works	**3 (3.1 GHz)**	**20.9%**	**1**	$\mathbf{0.75 \times 0.40}$	$\mathbf{< -20, (2.92f_0)}$
	5 (3.1 GHz)	**20.2%**	**1**	$\mathbf{0.75 \times 0.40}$	$\mathbf{< -20, (2.95f_0)}$

4. CONCLUSION

In this letter, two novel bandpass filters with improved selectivity based on only a ring resonator are proposed. Two/four transmission zeros close to the passband can be adjusted conveniently changing the even/odd-mode of the coupled lines. The proposed bandpass filters have advantages of high selectivity, higher passband-order and wideband harmonic suppression. Good agreements between simulated and measured responses of the filter are demonstrated, indicating good candidates for wideband wireless applications.

ACKNOWLEDGMENT

This work is supported by the 2012 Distinguished Young Scientist awarded by the National Natural Science Foundation Committee of China (61225001), and by National Natural Science Foundation of China (6140010914), Natural Science Foundation of Jiangsu Province (BK20140791) and the 2014 Zijin Intelligent Program of Nanjing University of Science and Technology.

REFERENCES

1. Wolff, I., "Microstrip bandpass filters using degenerate modes of a microstrip ring resonators," *IET Electron. Lett.*, Vol. 8, 163–164, 1972.
2. Chang, K. and L.-H. Hsieh, *Microwave Ring Circuits and Related Structures*, Wiley, New York, 2004.
3. Hong, J. S. and S. Li, "Theory and experiment of dual-mode microstrip triangular patch resonators and filters," *IEEE Trans. Microw. Theory Techn.*, Vol. 52, 1237–1243, 2004.
4. Zhang, X. Y. and Q. Xue, "Novel dual-mode dual-band filters using coplanar-waveguide-fed ring resonators," *IEEE Trans. Microw. Theory Techn.*, Vol. 55, 2183–2190, 2007.
5. Sun, S. and L. Zhu, "Wideband microstrip ring resonator bandpass filters under multiple resonances," *IEEE Trans. Microw. Theory Techn.*, Vol. 55, 2176–2182, 2007.
6. Feng, W., W. Q. Che, Y. L. Ma, and Q. Xue, "Compact wideband differential bandpass filter using half-wavelength ring resonator," *IEEE Microw. Wireless Compon. Lett.*, Vol. 23, 81–83, 2013.
7. Gómez-García, R., J. I. Alonso, and D. Amor-Martin, "Using the branch line directional coupler in the design of microwave bandpass filters," *IEEE Trans. Microw. Theory Techn.*, Vol. 53, 3221–3229, 2005.

8. Kim, C. H. and K. Chang, "Ultra-wideband (UWB) ring resonator bandpass filter with a notched band," *IEEE Microw. Wirel. Compon. Lett.*, Vol. 21, 206–208, 2011.
9. Feng, W., W. Q. Che, and Q. Xue, "Compact ultra-wideband bandpass filters with notched bands based on transversal signal-interaction concepts," *IET Microw. Antennas Propag.*, Vol. 7, 961–969, 2013.
10. Zhu, L. and K. Wu, "A joint field/circuit design model of microstrip ring dual-mode filter: Theory and experiments," *Asia-Pacific Microwave Conf.*, 865–868, 1997.
11. Yang, C. L., M. C. Chiang, H. C. Chiu, and Y. C. Chiang, "Design and analysis of a tri-band dual-mode chip filter for 60-, 77-, and 100-GHz applications," *IEEE Trans. Microw. Theory Tech.*, Vol. 60, No. 4, 989–997, Apr. 2007.
12. Luo, S., L. Zhu, and S. Sun, "A dual-band ring-resonator bandpass filter based on two pairs of degenerate modes," *IEEE Trans. Microw. Theory Tech.*, Vol. 58, No. 12, 3427–3432, Dec. 2010.
13. Chiang, Y.-C. and J.-P. Chen, "Design of miniature tri-band filter with multiple types of resonators," *Proc. Eur. Microw. Week*, Nuremberg, Germany, Oct. 6–11, 2013,
14. Guan, X., F. Yang, H. Liu, and L. Zhu, "Compact and high-isolation diplexer using dual-mode stub-loaded resonators, but high isolation," *IEEE Micro. Wireless Comp. Lett.*, Vol. 24, No. 6, 385–387, Jun. 2014.
15. Salleh, M., G. Prigent, O. Pigaglio, and R. Crampagne, "Quarter-wavelength side-coupled ring resonator for bandpass filters," *IEEE Trans. Microw. Theory Techn.*, Vol. 56, 156–162, 2008.
16. Khan, Z., M. Salleh, and N. Z. Zakaria, "Series-cascaded rings dual-band filter," *2010 Asia-Pacific Microwave Conference (APMC)*, 1758–1760, 2010.
17. Matthaei, G., L. Young, and E. M. T. Jones, *Microwave Filters, Impedance Matching Networks and Coupling Structures*, Artech House Inc, Norwood, MA, 1985.